Journal Pre-proof

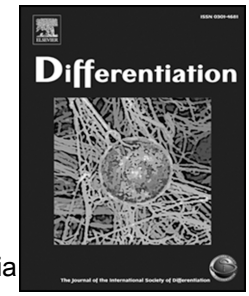

Characterizing the lens regeneration process in *Pleurodeles waltl*

Georgios Tsissios, Gabriella Theodoroudis-Rapp, Weihao Chen, Anthony Sallese, Byran Smucker, Lake Ernst, Junfan Chen, Yiqi Xu, Sophia Ratvasky, Hui Wang, Katia Del Rio-Tsonis

PII: S0301-4681(23)00013-0

DOI: https://doi.org/10.1016/j.diff.2023.02.003

Reference: DIFF 708

To appear in: *Differentiation*

Received Date: 14 September 2022

Revised Date: 6 February 2023

Accepted Date: 21 February 2023

Please cite this article as: Tsissios, G., Theodoroudis-Rapp, G., Chen, W., Sallese, A., Smucker, B., Ernst, L., Chen, J., Xu, Y., Ratvasky, S., Wang, H., Del Rio-Tsonis, K., Characterizing the lens regeneration process in *Pleurodeles waltl*, *Differentiation* (2023), doi: https://doi.org/10.1016/j.diff.2023.02.003.

Characterizing the lens regeneration process in *Pleurodeles waltl*

Georgios Tsissios [a, b, c, 1], Gabriella Theodoroudis-Rapp [a, 1], Weihao Chen [b, c, d], Anthony Sallese [a, b], Byran Smucker [b, e], Lake Ernst [a], Junfan Chen [f], Yiqi Xu [a], Sophia Ratvasky [a, b, c], Hui Wang [b, d], Katia Del Rio-Tsonis [a, b, c, *]

[1]Authors contributed equally to the manuscript
*Corresponding author

[a] Department of Biology Miami University, Oxford, OH, USA
[b] Center for Visual Sciences at Miami University, Oxford, OH, USA
[c] Cellular Molecular and Structural Biology Program, Miami University, Oxford, OH, USA
[d] Department of Chemical, Paper and Biomedical Engineering, Miami University, Oxford, OH, USA
[e] Department of Statistics, Miami University, Oxford, OH, USA
[f] Department of Chemistry and Biochemistry, Miami University, Oxford OH, USA

Keywords: *Lens regeneration, iPECs, aging, SD-OCT, cell cycle, ECM remodeling*

Corresponding author: Department of Biology, Miami University, 700 East High Street, Oxford, OH 45056, USA. Tel: (513) 529 3128, Email: delriok@miamioh.edu

Declaration of interest: None

Abstract

Background: Aging and regeneration are heavily linked processes. While it is generally accepted that regenerative capacity declines with age, some vertebrates, such as newts, can bypass the deleterious effects of aging and successfully regenerate a lens throughout their lifetime.
Results: Here, we used Optical Coherence Tomography (OCT) to monitor the lens regeneration process of larvae, juvenile, and adult newts. While all three life stages were able to regenerate a lens through transdifferentiation of the dorsal iris pigment epithelial cells (iPECs), an age-related change in the kinetics of the regeneration process was observed. Consistent with these findings, iPECs from older animals exhibited a delay in cell cycle re-entry. Furthermore, it was observed that clearance of the extracellular matrix (ECM) was delayed in older organisms.
Conclusions: Collectively, our results suggest that although lens regeneration capacity does not decline throughout the lifespan of newts, the intrinsic and extrinsic cellular changes associated with aging alter the kinetics of this process. By understanding how these changes affect lens regeneration in newts, we can gain important insights for restoring the age-related regeneration decline observed in most vertebrates.

1. Introduction

Aging can cause a myriad of intrinsic and extrinsic cellular changes, including but not limited to, mitochondrial dysfunction, telomere attrition, epigenetic modifications, proteostasis impairment, as well as ECM and cell adhesion alterations (López-Otín et al., 2013; Sharpless and DePinho, 2007; Xiao et al., 2015, Gorgoulis et al., 2019, Schumacher, 2009; Warraich et al., 2020;

Yousefzadeh et al., 2021). Consequently, these cellular changes lead to physiological imbalance, immune system dysfunction, tissue and organ degeneration, disease vulnerability, and decline in regeneration capacity (Ring et al., 2022).

Humans cannot yet escape these age-related consequences (Gardiner, 2005; Xiao et al., 2015). However, regenerative competent species, like newts, show negligible signs of aging and retain tremendous regenerative abilities even at an older age (Arenas Gómez and Echeverri, 2021; Brockes and Kumar, 2008; Joven et al., 2019; Sánchez Alvarado and Tsonis, 2006; Sousounis et al., 2014b). In fact, to test the extent to which newts can regenerate, a series of truly astonishing studies were conducted, where newt lenses were surgically removed up to 19 times over the period of 18 years from the same animals. By the time the final lenses were removed, the animals were 32 years old, and yet still regenerated complete lenses (Eguchi et al., 2011; Sousounis et al., 2015). When compared at the transcriptomic level, no significant differences were observed between the lenses collected from the animals that have undergone lens regeneration multiple times and the lenses from animals that had never undergone regeneration (Sousounis et al., 2015). Interestingly, when tails from the same animals that had never undergone regeneration were compared with tails collected from younger animals, thousands of genes associated with aging were found to be differentially regulated. Most noticeable, electron transport chain-associated genes were found to be downregulated in older tails, an indicative sign of mitochondrial dysfunction and metabolic alterations.

It is worth noting here that axolotls and frogs are also capable of regenerating their lens but lose this ability soon after embryonic development and metamorphosis respectively (Henry and Tsonis, 2010; Suetsugu-Maki et al., 2012; Vergara et al., 2018). When the iris of young axolotls, which serves as the source for lens regeneration, was compared at the molecular level with the iris of older regeneration incompetent axolotls, signs of aging were evident. Similar to newt aging tails, genes associated with electron transport chain, cell cycle, and DNA repair were significantly downregulated in the iris of old axolotls compared to young regeneration-competent animals (Sousounis et al., 2014a).

Based on the aforementioned studies, it is tempting to speculate that the initiation of regeneration triggers the rejuvenation of tissues and the surrounding microenvironment. However, the mechanism by which regenerative-competent animals avoid aging hallmarks to proceed with regeneration remains unclear. Understanding how aging affects cells at the cellular and extracellular levels in regeneration-competent animals is vital in our quest towards developing treatments for regenerative medicine and age-related pathologies. This is the first study to delineate the differences in cellular mechanisms (clearance of extracellular matrix) and kinetics on lens regeneration across three developmental stages of *Pleurodeles walt*l: pre-metamorphic larvae, post-metamorphic juvenile, and adult. Using live imaging (OCT), cell proliferation assays (EdU labeling) and ECM staining, we investigated the early stages of lens regeneration in which iPECs reprogram to switch cell fate and become lens cells. We also analyzed the later stages where the lens vesicle develops into a mature lens using 3D OCT imaging/processing and a statistical model to predict lens volume.

2. Materials and methods

2.1. Animal Handling and Ethical Statement

All experiments described in this study were executed under the guidelines provided by the Institutional Animal Care and Use Committee (IACUC) at Miami University. *Pleurodeles walt*l newts were housed in a homemade aquatic circulating system and daily care was performed following previously established husbandry guidelines (Joven et al., 2015). Environmental conditions such as temperature, feeding frequency, light cycle, water parameters and cleaning procedures were kept the same for all three age groups (Supplementary Table 1).

2.2 Surgical Procedures

Surgical removal of lens (lentectomy) and eye enucleation surgeries were performed as described before (Tsissios et al., 2022). Briefly, using a scalpel, a cut was made through the cornea and the lens was carefully removed with fine tweezers. For enucleations, the entire eyeball was removed by cutting the muscles and membranes around the sclera. The three age groups of *Pleurodeles walt*l consisted of: 2-month-old pre-metamorphic larvae, 6-month-old post-metamorphic juveniles, and 3-year-old post-metamorphic adults.

2.3 Spectral-Domain Optical Coherence Tomography

A customized Spectral-Domain Optical Coherence Tomography (SD-OCT) was used to follow the lens regeneration process from the same animals. For a detailed description of the SD-OCT setup, refer to Chen et al. (2021). In brief, a broadband light source centered at 850 nm was used in the SD-OCT setup, which can provide ~5 µm axial resolution and 7.5 µm lateral resolution respectively. A total of 2048 A-Scans were captured in each B-Scan, and 500 orthogonal positions across the lens were scanned to reconstruct a 3D image. Prior to imaging, newts were anesthetized and placed on a customized stage to avoid involuntary motion.

2.4 Live Imaging and Three-Dimensional Reconstructions

A total of 6 animals (12 eyes) were followed by OCT for 356 days. At first, images were taken every other day from day 0 until 28 days post-lentectomy (dpl) in order to capture all the dynamic changes that occur during the early stages of lens regeneration. Afterward, OCT imaging was performed every 5 days up until 88 dpl, and then every 50 days up until 365 dpl. B-scan images were cropped and rescaled to the accurate ratio according to the scanning distance of each individual eye. Then, the C-Scan stacks were reconstructed using B-Scans, and the lens tissue was segmented separately to synthesize the color label depicted in Fig. 2.

2.5 EdU Injections, Histology, and Cytochemistry

Newt eyes were collected at 1, 4,10, and 15 dpl for histological examination. At 24 hours prior to collection, EdU (Invitrogen, #C10338) was added intraperitoneal at 10 ug/g of body weight. Following eye enucleation, the entire eyeball was fixed in 10% formalin overnight at 4 ℃ and paraffin embedding was performed as described previously (Tsissios et al., 2022). Histological sections of 10 µm thickness were obtained and EdU and picrosirius red staining (Polysciences, #24901) were performed according to the manufacturer's protocol.

2.6 EdU Quantification and Statistical Analysis

The cell cycle re-entry experiment included the effects of two factors on the ratio of EdU+ to Hoechst stained cells: age (larvae, juvenile, adult) and time (1, 4, 10, and 15 dpl). For each of the twelve combinations of the two factors, six eyes were processed, leading to a total of 72 experimental units. We assumed that each of the eyes were independent. Though there could be a concern regarding the use of two eyes from the same organism, Yamada and Roesel (1969) have shown that iPECs of the contralateral uninjured eye do not re-enter the cycle as part of a systemic response. We also show that we have adequate power to detect scientifically relevant effects, even with as few as three replications per treatment (Supplementary File 2). Cells from nine cross-sections for each eye were counted, and the total number of EdU+/ Hoechst cells in both the dorsal and ventral iris were used in the statistical analysis. (For one of the larvae 4 dpl units, the data from a single cross-section was unusable; in this case, we simply proceeded with the remaining eight cross-sections.) Though it is standard in these types of studies to perform an ANOVA-type analysis (Inoue, 2012; Johnson, 2018; Como, 2023), because our measurements are counts, a more appropriate statistical analysis is based on the negative binomial distribution (Lindén and Mäntyniemi, 2011; Ver Hoef and Boveng, 2007; White and Bennetts, 1996). We provide more detailed reasons for our statistical modeling choice in Supplementary File 2, Section 3. Thus, a negative binomial regression, with two factors (day and time), as well as the interaction between the two factors, was used to model the number of EdU+ cells. Additionally, the number of Hoechst+ cells was included as the offset, which allows us to model the ratio of EdU+ to Hoechst+ cells. Using the interaction model with offset, the adult ratio was compared to the larvae and juvenile ratios, at each of the four time points, leading to a total of eight comparisons. The eight p-values were adjusted by controlling the False Discovery Rate (Benjamini and Hochberg, 1995). Supplementary File 2 provides more detailed discussion of the model and tests we performed, while also justifying the size of our study by a power analysis.

2.7 Lens Volume Quantification and Statistical Analysis

The volume of the lens was measured with SD-OCT as described before (Chen et al., 2021). The same SD-OCT images that were obtained from section 2.4 were used to calculate the volume. Each eye is assumed to be independent of every other eye, with two animals and thus four eyes in each age category (larvae, juvenile, and adult). We recognize that the assumption of independence of both eyes from an organism may not hold; we refer interested readers to a more detailed discussion in Supplementary File 1, where we give evidence that this is not a great concern to our conclusions. Each eye was imaged every other day from 0 to 28 dpl, as well as on day 33 and day 48, for a total of 14 measurements. One of the larvae animals died at 26 dpl, therefore lens volume after that time point was not included in the analysis. For each image, the volume of the lens was estimated, along with the diameter of the eye using the sectioning feature of ImageJ software. There are several aspects of this data that make it challenging to analyze. First, the trajectories are not easily modeled with standard polynomials (see Fig. 3A). Second, the measurements over time on a particular eye cannot be assumed independent; they are likely correlated. Third, the variation in the data was smaller early in the regeneration process. To address the first problem, Generalized Additive Models were used, to provide great flexibility to model nonstandard mean structures (Yee and Mitchell, 1991; Wood, 2006). For the second issue, a Generalized Additive Mixed Model (GAMM) was fitted via the gamm function in the mgcv R package in order to account for the correlation between measurements on a particular eye across time (Wood, 2006; 2022). In particular, a continuous autoregressive error structure (corCAR1) was used which estimates the level of correlation between successive measurements and

assumes that the correlation declines as the measurements get further away in time (Pinheiro and Bates, 2000). For the third concern, we modeled the natural log of the volume which stabilized the variance. The GAMM that we fit included smooth estimates of the mean log(Volume) for each level of age while accounting for the diameter variable in the model as well. More discussion of the intuition behind GAMMs, along with additional details regarding the fitting and results, are provided in Supplementary File 1.

3. Results

3.1 Real-time monitoring of lens regeneration in adult, juvenile, and larvae newts

We utilized SD-OCT to follow the process of newt lens regeneration in the three different age groups. We first imaged the intact eyes. Due to the unique light scattering properties of different ocular tissues we were able to visualize several anterior structures such as cornea, iris epithelium, stroma, lens epithelia and lens fibers (Fig. 1 D-F). Before lens removal, apart from the obvious size variations, no morphological or gross-anatomical differences were observed in the eyes between the three age groups with SD-OCT imaging (Fig. 1 D-F).

Lentectomy causes the loss of the aqueous humor and disruption between the anterior and posterior eye chambers. As a result, the anterior chamber is filled with ECM. Interestingly at 2 dpl, ECM filled the anterior chamber of the juvenile and adult animals compared to the larvae (Fig. 1 G-I). At this time point, the cornea appeared thicker in all three age groups compared to the corresponding cornea of the intact eye, indicating that proliferation to close the wound has started. By 4 dpl, the cornea appeared healed in larvae but not in juvenile and adult animals (Supplementary Fig. 1 A-C). At 6 dpl, the ECM in the anterior chamber of the larvae animals mostly cleared out and a transparent chamber was established (Supplementary Fig. 1 D). On day 8, iPECs, located at the tip of the dorsal iris of larvae animals, have depigmented and switched cell fate to become lens cells. These cells then formed an immature, asymmetrical lens vesicle (Fig. 1 J). By 12 dpl, the cornea of the juvenile has healed, and a clear anterior chamber mostly devoid of ECM was observed (Supplementary Fig. 1 K). Later, at 14 dpl, a lens vesicle was visible in the juvenile newt eye (Fig. 1 N). As lens morphogenesis proceeds in larvae animals, elongated lens cells fill the lumen of the lens. These cells are called primary lens fibers and are arranged in a concentric fashion in the middle of the lens, whereas the cuboidal lens epithelial cells are arranged in a monolayer at the periphery of the lens (Fig. 1 M). In adults, ECM did not completely clear until 22 dpl, and a lens vesicle appeared soon after at 24 dpl (Supplementary Fig. 1 X, Fig. 1 R).

During further growth, lens epithelial cells at the equatorial region of the lens differentiate and give rise to secondary lens fibers that surround the previously formed primary fibers. These newly formed lens fibers have different organelle compositions compared to primary lens fibers that have lost all organelles. The difference in organelle composition results in different scattering properties and therefore can be distinguished by SD-OCT (Fig. 1 T; Supplementary Fig. 1 Y, Aj) (Gupta et al., 2020). Eventually, the regenerating lens buds off from the dorsal iris to regain its original position. This is an essential step for regaining functional vision and a signal to mark the end of the regeneration process. In larval animals, the lens appeared detached from the dorsal iris at 58 dpl, and 78 dpl in juvenile animals (Fig. 1 S; Supplementary Fig. 1 Ai,). Surprisingly, even at 365 dpl, the adult lens was still attached to the dorsal iris (Fig. 1 X).

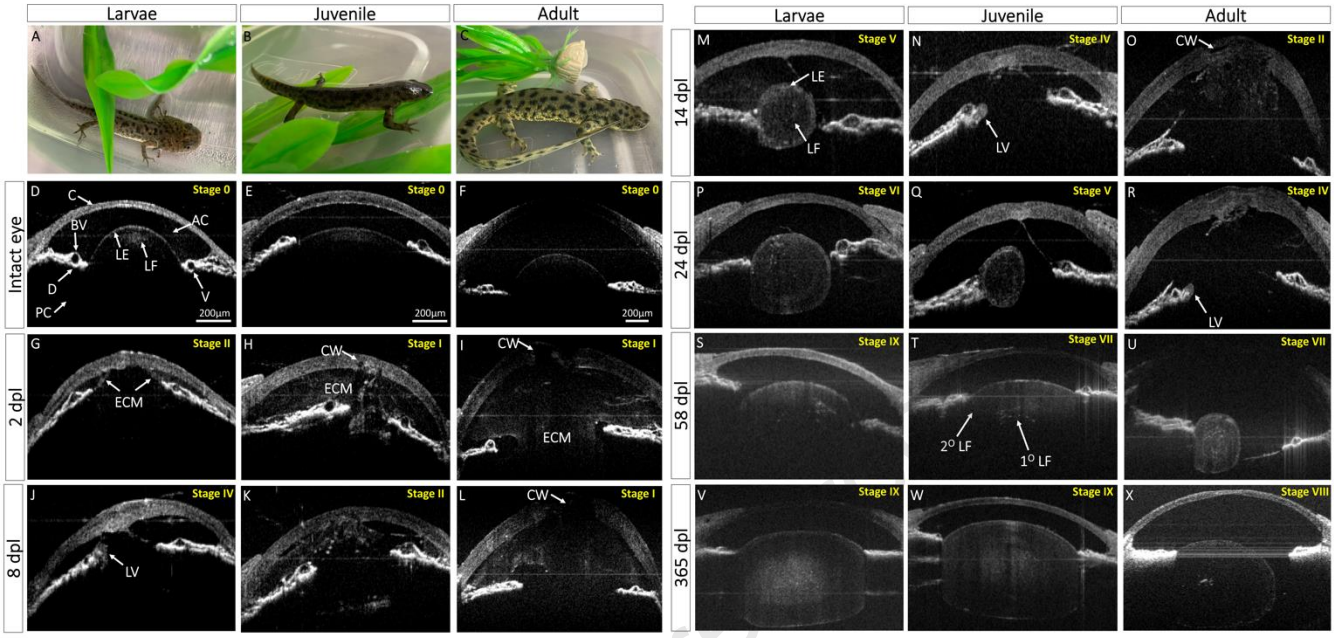

Fig. 1: *In vivo* monitoring of lens regeneration from larval, juvenile, and adult newts**. (A-C)** Pictures of larvae, juvenile and adult *P. waltl.* **(D-X)** B-scan images are shown here in grayscale images. Eyes were kept at the same orientation for all time points, with cornea (C) at the anterior, dorsal iris (D) on the left side, and ventral iris (V) to the right of the image. This figure depicts the timing of morphological events that occur during lens regeneration in each age group such as healing of cornea wound (CW), extracellular matrix (ECM) remodeling in the anterior (AC) and posterior chambers (PC), lens vesicle (LV) appearance, primary lens fiber (1^{o}LF) differentiation from the epithelial cells of the lens vesicle, and lens epithelial differentiation into secondary lens fibers (2^{o}LF). Approximate lens regeneration stages according to Sato (1940) are depicted on the top right of each OCT image.

3.2 Three-dimensional view of lens morphogenesis

Three-dimensional SD-OCT images compiled from cross-sectional B-scans were used to acquire a multi-angle, panoramic view of the entire anterior eye. The first appearance of a lens vesicle (shown in red) was evident at 8 dpl from the mid-dorsal margin of the iris epithelium of larval animals, whereas a lens vesicle was noticeable at 14 dpl and 24 dpl in juveniles and adults respectively (Fig. 2A, E, I). As the iris to lentoid transition takes place, the newly formed lens vesicle appears in an irregular, asymmetric and hollow shape. By 14 dpl in the larvae and 24 dpl in the juvenile, lens epithelial cells at the equatorial region of the regenerating lens elongate and differentiate into lens fibers, resulting in a larger and more symmetric lens (Fig. 2 D, H, Suppl. movie 1). As the regenerating lens continues to develop, newly formed secondary lens fibers symmetrically enclose the primary lens fibers, and the lens appears larger and more spherical at 24 dpl in the larvae. (Fig. 2G, Suppl. movie 1).

3.3 Growth rates of the regenerating lens

SD-OCT was used to quantify lens volume, and mean growth rates of the regenerating lenses were estimated using a Generalized Additive Mixed Model. The experiment makes it clear that

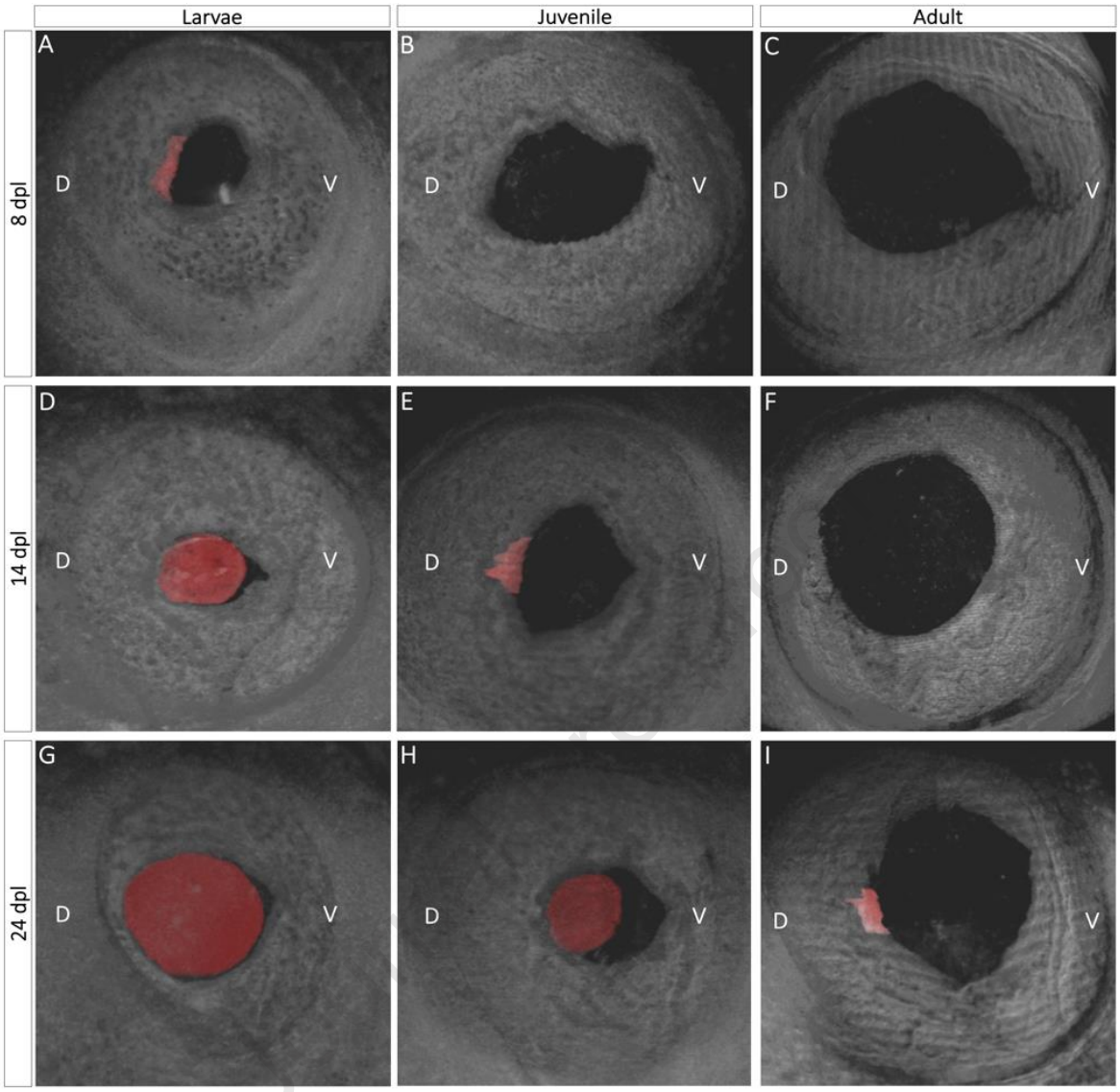

Fig. 2: Three-dimensional view of lens regeneration**.** B- scans were used to reconstruct a three-dimensional image of the newt eye. To aid in visualization, the regenerating lens was pseudo-colored with red color. Three-dimensional images permit detailed observations of lens growth and morphogenesis. When it first appears, the lens vesicle is located in the mid-dorsal region of the iris and has an asymmetrical shape (A, E, I). As the lens develops and more lens epithelial cells differentiate into lens fibers, the regenerating lens assumes a spherical shape (D, G, H).

the time by which the lens begins to grow is associated with age (Fig. 3A). Once the growth begins, however, the trajectories of juvenile and adult were very similar. On the other hand, there is evidence that the larvae trajectory for lens growth is different from both the juvenile and adult (Fig. 3B; $p < 0.001$) when comparing the larvae to the other two smoothed curves. For example, when measuring from the time point when growth was detected, the larvae started off smaller but quickly accelerated past juveniles and adults in terms of size. Because of the relatively small study and the approximate nature of the GAMM inference, we recognize these conclusions as tentative.

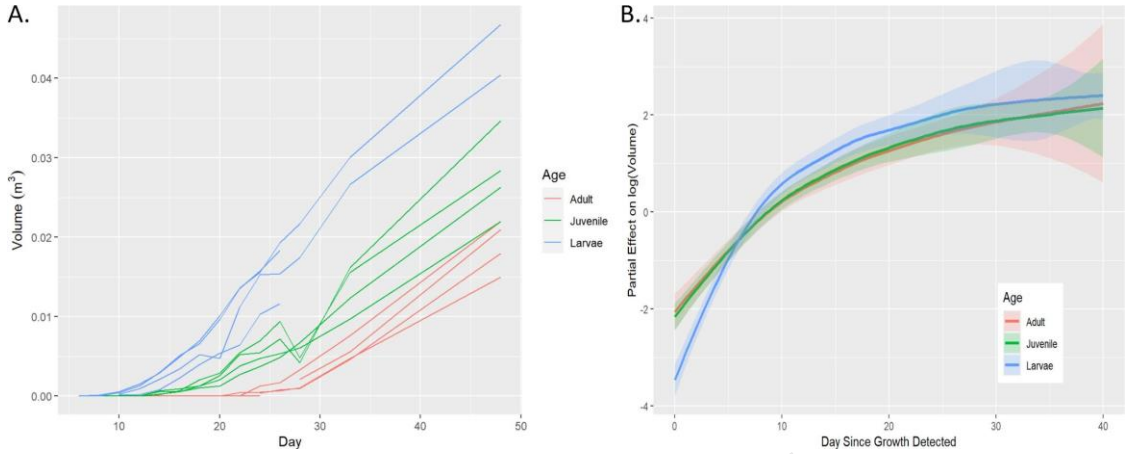

Fig. 3: Comparisons of lens growth rates between three age groups. **A:** SD-OCT images were used to calculate the volume of lens vesicles from the time they appeared until 48 dpl. The raw volume data is plotted across the day of the experiment. **B:** A Generalized Additive Mixed Model (GAMM) was used to estimate the effect of the three groups on lens log(Volume) once the lens vesicle appears.

3.4 iPECs cell cycle kinetics

Prior to lentectomy, iPECs are terminally differentiated and rest in G_0 (Supplementary Fig. S2). EdU+ cells were observed in the iris epithelium and stroma of larval animals as early as 1 dpl (Fig. 4A, B). At 4 dpl, cell cycle entry was evident in juvenile newts but at a much higher rate in larval animals. Once the lens formed, in larvae, iPECs that did not transdifferentiate to become lens cells withdrew from the cell cycle, and eventually returned to near baseline levels at 15 dpl (Fig. 4A, B). The cells that transdifferentiated into lens and formed lens vesicles continued to proliferate but were not included in the iPECs quantification depicted in Fig 4B. A significant delay in the iPECs cell cycle entry was observed in the adult eye, and no signs of fully depigmented iPECs were noticeable during the first 15 days.

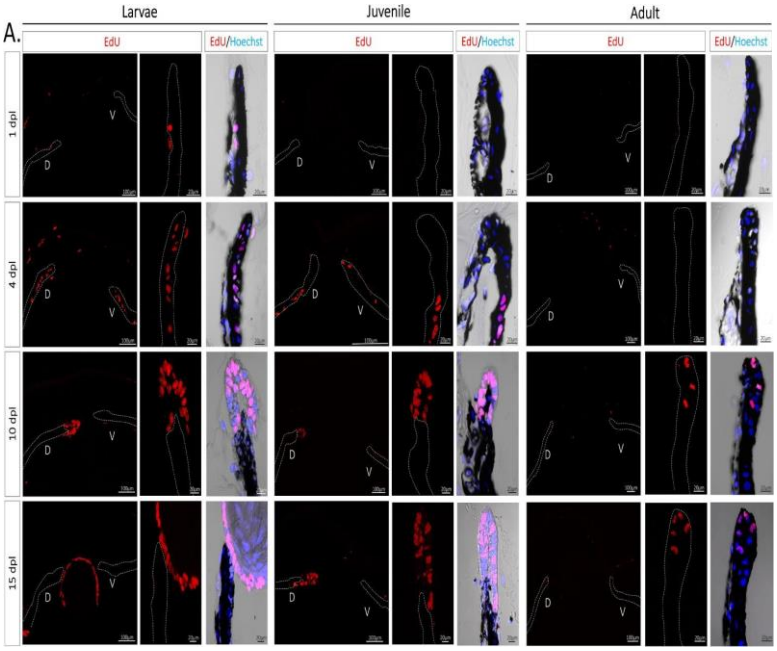

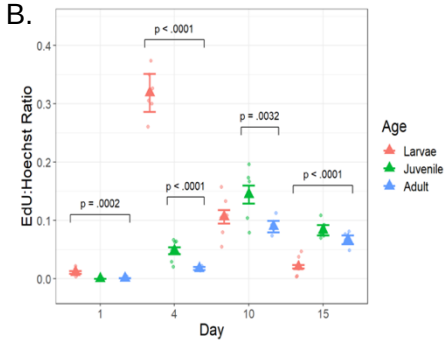

Fig. 4: Histological examination and quantification of cell cycle dynamics during lens regeneration. **A:** EdU staining was performed to explore differences in cell cycle re-entrance and progression of the iris pigment epithelium between the three age groups. EdU+ cells were observed in the iris epithelium (dotted line) and stroma of larval eyes at 1 dpl and in higher numbers at 4 dpl. By 10 dpl EdU+ cells were observed in the newly formed lens vesicle. EdU+ cells were found at 4 dpl in juvenile eyes and not until 10 dpl in adult eyes in the iris pigment epithelium. **B:** The ratio of the number of iris epithelial EdU+ cells to Hoechst+ cells was plotted along the y-axis vs the day of lentectomy on the x-axis. Raw data (points) estimated mean ratio (triangle), and error bars using the standard error of the estimates are all displayed in the graph. Among the eight within-day comparisons with adult eyes, those with small FDR-adjusted p-values are annotated; none of the other three had p-values less than 0.2. For A only the middle cross-section of each eye is shown, whereas in B a total of 9 cross-sections covering the entire area of the eye were used for quantification.

3.5 Collagen synthesis and remodeling during lens regeneration

Collagen staining was performed to confirm SD-OCT observations about ECM remodeling during regeneration. At 1 dpl, juvenile and adult eyes showed picrosirius red staining in the anterior and posterior chambers, indicating a homogenous presence of dense collagen fibers and sheets in the entire eye (Fig. 5). However, this was not the case in larval newts, as non- homogeneous collagen staining was observed throughout the eye cavity. In the anterior chamber, collagen appeared compacted, whereas collagen presence was less dense in the rest of the eye (Fig. 5). Collagen remodeling took place in the larvae eyes at 4 dpl, and by 10 dpl, most collagen was cleared out from the anterior chamber. Juvenile newts depicted clearing of most of the collagen at 15 dpl in the anterior chamber, whereas in adult animals, the aqueous chamber still contained collagen even at 15 dpl when signs of collagen remodeling were observed.

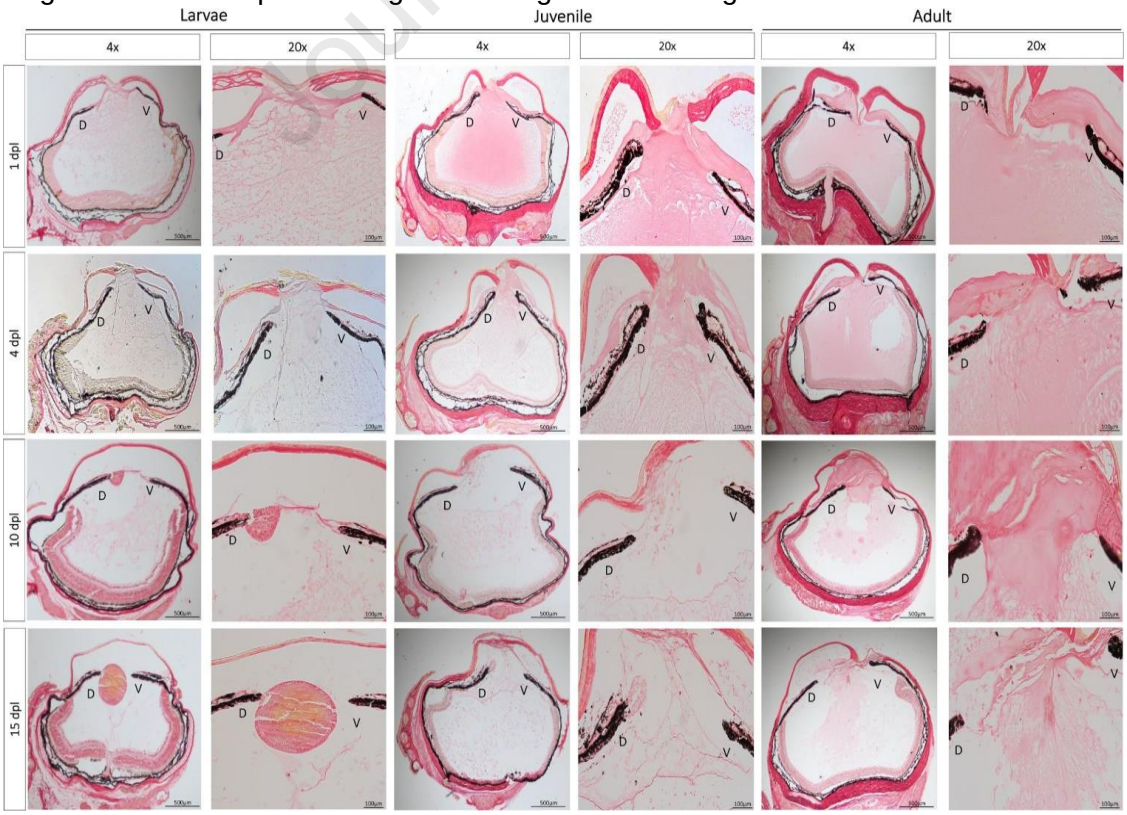

Fig. 5: Histological examination of ECM remodeling during the early stages of lens regeneration. Picrosirius red staining was performed to visualize collagen composition and distribution throughout the newt eye at different stages of lens regeneration. Breakdown of collagen fibers in the anterior chamber is evident as early as 1 dpl in larval animals and by 10 dpl almost all collagen is cleared out of the eye chamber. On the contrary, collagen staining was observed all over the eye cavity in juvenile and adult eyes at 1 dpl. The remodeling process occurs slower in adult animals, as evidenced by the collagen staining detected in the anterior chamber at 15 dpl. D= dorsal iris; V= ventral iris. Magnifications are shown in each figure (4x: 100 um; 20x: 500 um).

4. Discussion

In this study, we demonstrate that although the capacity for lens regeneration in *Pleurodeles waltl* is not lost with aging, the dynamics of this process is altered. Using *in vivo* imaging, we were able to follow the process of lens regeneration uninterrupted for 365 days from the same individuals and reported the morphological and cellular changes that occurred during the various stages of this process. We found that at the early stages of transdifferentiation, phenomena such as cornea healing, ECM remodeling, iPECs cell cycle re-entry, and lens vesicle appearance occurred faster in the pre-metamorphotic larvae compared to post-metamorphotic juvenile and adult animals. On the other hand, no clear differences were observed in the lens differentiation rate and morphogenesis during the late stages of lens regeneration.

Although the cellular events that govern lens regeneration have been previously described in newt species, such as *Notophthalmus viridescens* and *Cynops pyrrhogaster,* to our knowledge this is the first detailed report that characterized stages of lens regeneration in *Pleurodeles waltl* (Eguchi, 1963, 1964; Reyer, 1954; Vergara et al., 2018; Yamada, 1977). Tadao Sato categorized the process of lens regeneration into 13 distinct stages (Sato, 1930; 1935; 1940). We have matched Sato stages to our *P. waltl* lens regeneration stages (Fig.1, Supplementary Fig 1 and Fig. 6). In the early stages, iPECs undergo transdifferentiation to reprogram and become lens cells (Sato stages I-III). We also observed a drastic difference in the timing of lens vesicle appearance among the three age groups. A lens vesicle was detected as early as 8 dpl in larvae, 14 dpl in juvenile, and 24 dpl in adult animals. After a lens vesicle is formed, the mechanisms and events of lens growth and morphogenesis parallel those of eye development in vertebrates (Tsonis et al., 2004). At first, epithelial cells at the internal wall of the lens vesicle become elongated to form the primary lens fibers (Sato Stage V-VII). Sequentially, the epithelial cells at the equatorial region of the lens stop proliferating, begin to change shape, and then lose their organelles as they differentiate into lens fibers (Chaffee et al., 2014). These secondary lens fibers then migrate towards the center of the lens, where they will surround the previously formed primary fibers (Sato Stages VIII-XI). No obvious differences were observed regarding the events and rate of lens development and morphogenesis.

To further compare the rates of lens growth between larvae, juvenile and adult animals, three-dimensional SD-OCT images were utilized to quantify the volume of the regenerating lenses. The rate of lens growth between different developmental stages has been described before in several newt species (Reyer, 1954; Inoue et al., 2012). However, these studies acquired lens growth measurements from histological sections, which required sacrificing the animals at each time point. This method is not ideal and fails to account for the variability between individual newts. SD-OCT is a non-invasive method which allows us to continuously quantify the lens growth from

the same animal and without any tissue artifacts that are often introduced via histological processing (Chen et al., 2021). Consistent with our morphological observations, after the lens vesicle was formed, we observed similar rates of growth between juvenile and adult lenses, whereas the size of the larval lens was initially smaller but grew more rapidly until about 10 dpl.

During the late stages of lens regeneration, once the lens is mature and covers the entire pupil area (from dorsal to ventral iris), it detaches from the dorsal iris and relocates to its initial position in the middle of the eye where it is held by the zonule fibers (Tsonis et al., 2004). Interestingly, even though the rate of lens growth was not different, we observed a delay in lens detachment from the dorsal iris in older animals. In fact, even at 365 dpl, the lenses of adult newts were still attached to the dorsal iris. As our data displays a similar growth rate between age groups, we concluded that the reason the adult animal failed to reach the size of an intact lens by 365 dpl was not in fact due to differences in the speed of lens growth, but due to the fact that the size of the lens in adults are much bigger than the lens of younger animals. Therefore, it will take the aged newts a longer time to obtain the necessary size. The smaller the original lens, the faster the regenerating tissue will reach its original size.

The re-entrance of iPECs into the cell cycle is the most prominent and critical step during the early stages of lens regeneration. Under normal conditions, iPECs are terminally differentiated cells that show no signs of cell division (Eguchi and Shingai, 1971; Reyer, 1971; Yamada and Roesel, 1969; Zalik and Yamada, 1967, Yamada and McDevitt, 1974). Lentectomy reverts the differentiation status of these mature cells and triggers cell cycle re-entry. Cell cycle kinetics during lens regeneration have been well documented both *in vivo* and *in vitro* in a variety of newt species (Horstman and Zalik, 1974; Yamada et al., 1975; Zalik and Yamada, 1967). From these studies, it was concluded that iPECs from adult newts transition from G0 to G1 between 3-5 dpl and start to withdraw from the cell cycle once the lens vesicle is formed. Here we observed that cell cycle re-entry was faster and at a higher magnitude in larval animals. Surprisingly, we detected EdU + cells from the epithelium and stroma of the larval iris as early as 1 dpl. At 4 dpl, almost the entire dorsal and ventral iris was EdU positive. By 10 dpl, once the lens vesicle was formed, the EdU:Hoechst ratio was decreased as the iPECs withdrew from the cell cycle and regained their original identity. In contrast, very few EdU+ IPECs were observed in adult eyes at 10 and 15 dpl. Furthermore, no signs of depigmentation were observed until 15 dpl. One possible explanation for the age-related cell cycle re-entrance delay that we observed is that the differentiation status of iPECs is more advanced in adult animals, causing the dedifferentiation process to take longer. Future work should explore the molecular signatures of iPECs from young and old animals during lens regeneration, in order to provide age-related differences in differentiation trajectories and cell fate decisions. It is also interesting to note here, that when the process of lens regeneration was investigated in outer space, an environment known to cause anti-aging effects in humans, cell cycle re-entry was faster and at a higher magnitude when compared to newts that were kept on Earth (Grigoryan et al., 2002; Grigoyan and Radugina, 2019; Otsuka et al., 2021). Further exploring the association between microgravity, aging, and cell cycle acceleration could provide important insights into the aging effects of iPECs seen in this study.

The composition and remodeling of ECM is a fundamental aspect of wound healing and critical determinant of the regeneration outcome (Erickson and Echeverri, 2018). Failure to remodel ECM during the early steps of wound healing leads to scar formation, whereas the dynamic degradation of ECM proteins is often associated with regeneration success (Arenas Gómez et al., 2020;

Huang et al., 2021; Satoh et al., 2011; Seifert et al., 2012; Vinarsky et al., 2005). Despite the importance of ECM remodeling, very little is known about this process during lens regeneration. Through histological examination and electron microscopy studies, it has been shown that ECM accumulates into the anterior aqueous chamber immediately after lens removal (Tsonis et al., 2004; Yamada, 1977). Prior to lentectomy, the anterior chamber of the eye is filled with a transparent material that allows light to pass through and supports the function of lens epithelial cells. Following lentectomy, the transparent aqueous humor is lost, and the eye cavity fills with ECM. In this study, we used SD-OCT and picrosirius red staining to investigate the dynamic remodeling of ECM during regeneration and characterized age-related variations of this process. OCT imaging was previously validated as a powerful tool to detect real-time changes in ECM composition in several mammalian tissues (Carpaij et al., 2020; Yang et al., 2011). To the best of our knowledge, this is the first attempt to monitor ECM during lens regeneration *in vivo*. We observed across all three life stages that the lens vesicle did not develop until the ECM was cleared from the aqueous chamber. These results highlight the importance of ECM removal for successful regeneration. A possible explanation for the effects of ECM on regeneration is that it interferes with the trafficking of growth factors produced by the retina. It was previously shown that growth factors such as FGFs are produced and secreted from the retina, and that FGFs are necessary for lens regeneration in the newt eye (Caruelle et al., 1989; Del Rio- Tsonis et al., 1997; Del Rio-Tsonis et al., 1998; Hayashi et al., 2004). Therefore, we hypothesize that the presence of dense matrix proteins in the eye cavity can negatively impact the trafficking of growth factors secreted from the retina and used by the iPECs.

Collectively, we have shown that age delays the process of transdifferentiation during lens regeneration in *Pleurodeles waltl*. Unraveling the molecular mechanisms by which regeneration-competent animals circumvent the deleterious effects of aging and retain tremendous regenerative powers will make major inroads in the development of therapies to treat geriatric diseases.

Acknowledgments

The authors would like to thank Drs. Max Yun and Andras Simon from the Center for Regenerative Therapies in Dresden, Germany, and Karolinska Institute in Stockholm, Sweden for gifting us *Pleurodeles waltl* animals to start our colony at Miami University. Special thanks to Dr. Alberto Joven for his guidance in husbandry and breeding techniques. In addition, the authors thank Laboratory Animal Resources (LAR) director Jazzminn Hembree and the entire LAR team for their help to establish and maintain our colony. Moreover, further thanks to Matt Duley from the Center of Advanced Microscopy and Imaging (CAMI) at Miami University and Erika Grajales- Esquivel for their help and guidance on imaging procedures.

This research was supported by grants from the National Eye Institute: RO1 EY027801 (to KDRT) and R21 EY031865 (to HW and KDRT), by the John W. Steube Professorship Endowment (to KDRT), the Sigma Xi Aid in Research Grant (to GTR) and Miami University undergraduate research grants.

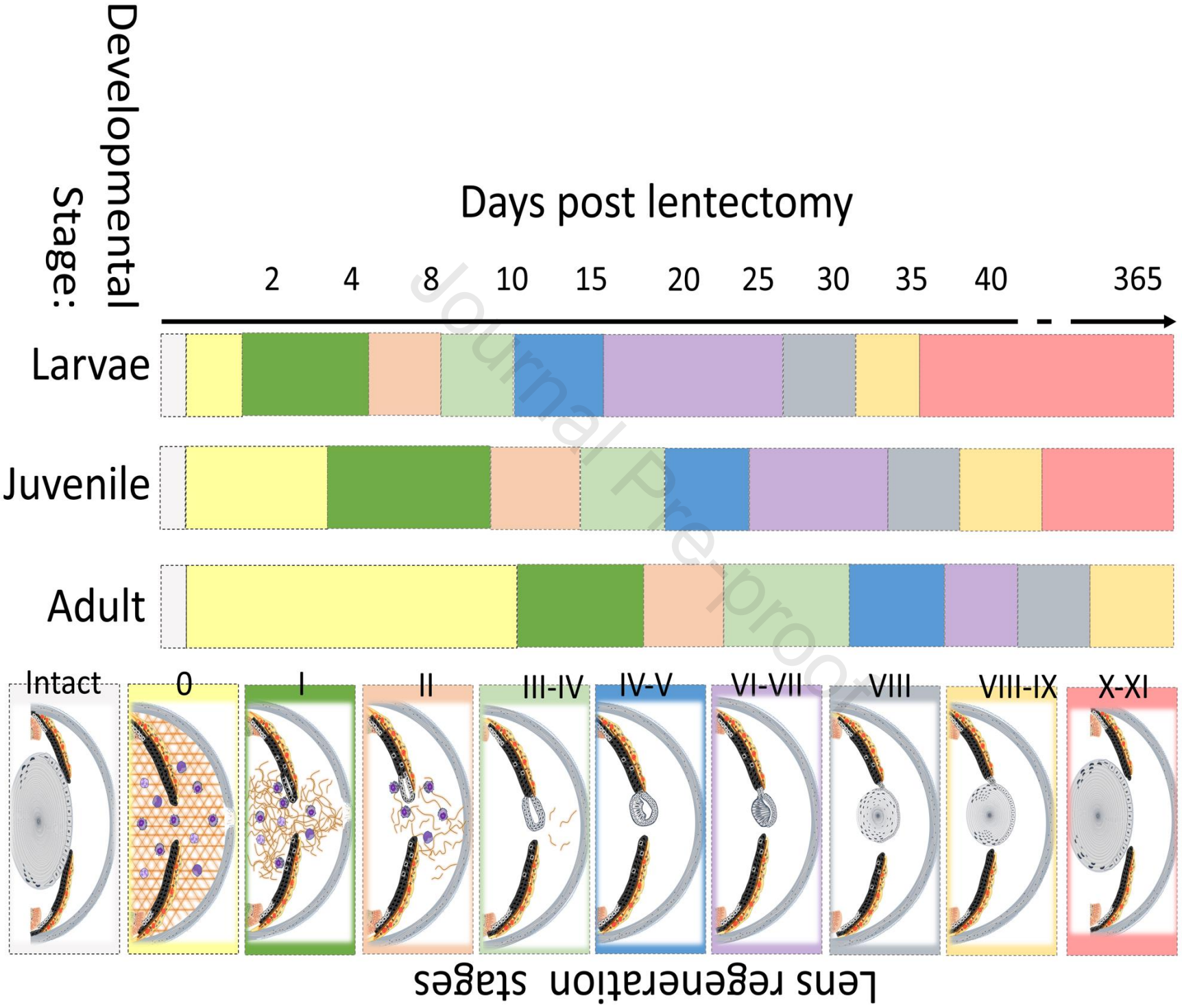

Fig 6. Graphical description of the proposed stages of lens regeneration in *Pleurodeles waltl*. Lens regeneration staging was modified from Sato's stages (Sato, 1940, Yamada, 1977). Prior to injury iPECs are terminally differentiated adult somatic cells and at rest in G_0. Following lentectomy, the aqueous and vitreous chambers are disrupted by lentectomy and fill with extracellular matrix (appears as condensed and compact fibers and sheets)[Sato's stage 0] . Also at this time immune and blood cells migrate into the injured area. Subsequently, the iPECs re-enter the cell cycle (transition from G_0 to G_1) [Sato's stage I]. Extracellular remodeling also starts at this time. Soon after, the iPECs at the tip of the dorsal iris become depigmented while extracellular matrix remodeling continues to takes place [Sato's I]. The depigmented iPECs proliferate and differentiate into lens cells giving rise to an early lens vesicle. These cells start synthesizing lens specific proteins such as Crystallins [Sato's stage III-IV] . At this time extracellular matrix is mostly removed from the eye chambers. Cells of the lens vesicle continue to proliferate. Cells located in the inner wall of the lens vesicle start to elongate [Sato's stage IV-VI]. The remaining iPECs that were partially depigmented start to withdraw from the cell cycle. As lens morphogenesis continues, internal cells differentiate into primary, and the lens epithelial cells on the anterior side proliferate [Sato's stage VI-VII]. Next, the primary lens fibers start to lose their nucleus and other organelles and assume a concentric arrangement [Sato's stage VIII]. Lens epithelial cells at the equatorial zone start to differentiate giving rise to secondary lens fibers. During this time, iPECs cease proliferation and start to resynthesize their melanosomes [Sato's stage VIII-IX]. Almost all lens fibers lose their nucleus and other organelles, except the newly formed fibers at the outer region near the lens equator. Regenerating lens detaches from the dorsal iris and assumes a position at the center of the eye [Sato's stage X-XI].

References

Arenas Gómez, C.M., Echeverri, K., 2021. Salamanders: The molecular basis of tissue regeneration and its relevance to human disease. Curr Top Dev Biol 145, 235-275.

Arenas Gómez, C.M., Sabin, K.Z., Echeverri, K., 2020. Wound healing across the animal kingdom: Crosstalk between the immune system and the extracellular matrix. Dev Dyn 249, 834-846.

Benjamini, Y., & Hochberg, Y., 1995. Controlling the false discovery rate: a practical and powerful approach to multiple testing. Journal of the Royal statistical society: series B (Methodological) 57(1), 289-300.

Brockes, J.P., Kumar, A., 2008. Comparative aspects of animal regeneration. Annu Rev Cell Dev Biol 24, 525-549.

Carpaij, O.A., Goorsenberg, A.W.M., d'Hooghe, J.N.S., de Bruin, D.M., van den Elzen, R.M., Nawijn, M.C., Annema, J.T., van den Berge, M., Bonta, P.I., Burgess, J.K., 2020. Optical Coherence Tomography Intensity Correlates with Extracellular Matrix Components in the Airway Wall. Am J Respir Crit Care Med 202, 762-766.

Caruelle, D., Groux-Muscatelli, B., Gaudric, A., Sestier, C., Coscas, G., Caruelle, J.P., Barritault, D., 1989. Immunological study of acidic fibroblast growth factor (aFGF) distribution in the eye. J Cell Biochem 39, 117-128.

Chaffee, B.R., Shang, F., Chang, M.L., Clement, T.M., Eddy, E.M., Wagner, B.D., Nakahara, M., Nagata, S., Robinson, M.L., Taylor, A., 2014. Nuclear removal during terminal lens fiber cell differentiation requires CDK1 activity: appropriating mitosis-related nuclear disassembly. Development 141, 3388-3398.

Chen, W., Tsissios, G., Sallese, A., Smucker, B., Nguyen, A.T., Chen, J., Wang, H., Del Rio-Tsonis, K., 2021. In Vivo Imaging of Newt Lens Regeneration: Novel Insights Into the Regeneration Process. Transl Vis Sci Technol 10, 4.

Como, C., Cervantes, C., Pawlikowski B., Siegenthaler, J., (2023). Retinoic acid signaling in mouse retina endothelial cells is required for early angiogenic growth. Differentiation 130, 16-27.

Del Rio-Tsonis, K., Jung, J.C., Chiu, I.M., Tsonis, P.A., 1997. Conservation of fibroblast growth factor function in lens regeneration. Proc Natl Acad Sci U S A 94, 13701-13706.

Del Rio-Tsonis, K., Trombley, M.T., McMahon, G., Tsonis, P.A., 1998. Regulation of lens regeneration by fibroblast growth factor receptor 1. Dev Dyn 213, 140-146.

Eguchi, G., 1963. Electron microscopic studies on lens regeneration. Embryologia 8, 45-62.

Eguchi, G., 1964. Electron microscopic studies on lens regeneration. Embryologia 8, 247-287.

Eguchi, G., Eguchi, Y., Nakamura, K., Yadav, M.C., Millán, J.L., Tsonis, P.A., 2011. Regenerative capacity in newts is not altered by repeated regeneration and ageing. Nat Commun 2, 384.

Eguchi, G., Shingai, R., 1971. Cellular analysis on localization of lens forming potency in the newt iris epithelium. Dev Growth Differ 13, 337-349.

Erickson, J.R., Echeverri, K., 2018. Learning from regeneration research organisms: The circuitous road to scar free wound healing. Dev Biol 433, 144-154.

Gardiner, D.M., 2005. Ontogenetic decline of regenerative ability and the stimulation of human regeneration. Rejuvenation Res 8, 141-153.

Gorgoulis, V., Adams, P.D., Alimonti, A., Bennett, D.C., Bischof, O., Bishop, C., Campisi, J., Collado, M., Evangelou, K., Ferbeyre, G., Gil, J., Hara, E., Krizhanovsky, V., Jurk, D., Maier, A.B., Narita, M., Niedernhofer, L., Passos, J.F., Robbins, P.D., Schmitt, C.A., Sedivy, J., Vougas, K., von Zglinicki, T., Zhou, D., Serrano, M., Demaria, M., 2019. Cellular Senescence: Defining a Path Forward. Cell 179, 813-827.

Grigoryan, E.N., Mitashov, V.I., Anton, H.J., 2002. Urodelean amphibians in studies on microgravity: effects upon organ and tissue regeneration. Adv Space Res 30, 757-764.

Grigoyan, E.N., Radugina, E.A. 2019. Behavior of Stem-Like Cells, Precursors for Tissue Regeneration in Urodela, Under Conditions of Microgravity. Stem Cells Dev 28, 423-437.

Gupta, A., Ruminski, D., Jimenez Villar, A., Duarte Toledo, R., Manzanera, S., Panezai, S., Mompean, J., Artal, P., Grulkowski, I., 2020. In vivo SS-OCT imaging of crystalline lens sutures. Biomed Opt Express 11, 5388-5400.

Hayashi, T., Mizuno, N., Ueda, Y., Okamoto, M., Kondoh, H., 2004. FGF2 triggers iris-derived lens regeneration in newt eye. Mech Dev 121, 519-526.

Henry, J.J., Tsonis, P.A., 2010. Molecular and cellular aspects of amphibian lens regeneration. Prog Retin Eye Res 29, 543-555.

Horstman, L.P., Zalik, S.E., 1974. Growth of newt iris epithelial cells in vitro: a study of the cell cycle. Exp Cell Res 84, 1-14.

Huang, T., Zuo, L., Walczyńska, K.S., Zhu, M., Liang, Y., 2021. Essential roles of matrix metalloproteinases in axolotl digit regeneration. Cell Tissue Res 385, 105-113.

Inoue, T., Inoue R., Tsutsumi, R., Tada, K., Urata, Y., Michibayashi, C., Takemura, S., and Agata, K., 2012. Lens regenerates by means of similar processes and timeline in adults and larvae of the newt Cynops pyrrhogaster. Developmental Dynamics 241, 1575–1583

Johnson, K., Batman, J., DiTommaso, T., Wong, A., Whited, J., (2018). Systemic cell cycle activation is induced following complex tissue injury in axolotl. Developmental Biology, 433(2), 461-472.

Joven, A., Elewa, A., Simon, A., 2019. Model systems for regeneration: salamanders. Development 146.

Joven, A., Kirkham, M., Simon, A., 2015. Husbandry of Spanish ribbed newts (Pleurodeles waltl). Methods Mol Biol 1290, 47-70.

Lindén, A., Mäntyniemi, S., 2011. Using the negative binomial distribution to model overdispersion in ecological count data. Ecology 92, 1414-1421.

López-Otín, C., Blasco, M.A., Partridge, L., Serrano, M., Kroemer, G., 2013. The hallmarks of aging. Cell 153, 1194-1217.

Otsuka, K., Cornelissen, G., Furukawa, S., Kubo, Y., Shibata, K., Mizuno, K., Ohshima, H., Mukai, C., 2021. Astronauts well-being and possibly anti-aging improved during long-duration spaceflight. Sci Rep 11, 14907.

Pinheiro, J.C., & Bates, D. M., 2000. Linear mixed-effects models: basic concepts and examples. Mixed-effects models in S and S-Plus. 3-56.

Reyer, R.W., 1954. Regeneration of the lens in the amphibian eye. Q Rev Biol 29, 1-46.

Reyer, R.W., 1971. DNA synthesis and the incorporation of labeled iris cells into the lens during lens regeneration in adult newts. Dev Biol 24, 533-558.

Ring, N.A.R., Valdivieso, K., Grillari, J., Redl, H., Ogrodnik, M., 2022. The role of senescence in cellular plasticity: Lessons from regeneration and development and implications for age-related diseases. Dev Cell 57, 1083-1101.

Sánchez Alvarado, A., Tsonis, P.A., 2006. Bridging the regeneration gap: genetic insights from diverse animal models. Nat Rev Genet 7, 873-884.

Sato, T., 1930. Beitriige zur Analyse der Wolffschen Linsenregeneration. Wilhelm Roux Arch Entwickl Mech Org 122, 451-493.

Sato, T., 1935. Beitriige zur Analyse der Wolffschen Linsenregeneration. III. Wilhelm Roux Arch Entwickl Mech Org 133, 323-348.

Sato, T.,1940 Vergleichende Studien ilber die Geschwindigkeit der Wolffschen Linsenregeneration bei Triton taeniatus und bei Diemyctylus pyrrhogaster. Arch. EntwMech. Org.140: 573-613.

Satoh, A., makanae, A., Hirata, A., Satou, Y., 2011. Blastema induction in aneurogenic state and Prrx-1 regulation by MMPs and FGFs in Ambystoma mexicanum limb regeneration. Dev Biol 355, 263-274.

Schumacher, B., 2009. Transcription-blocking DNA damage in aging: a mechanism for hormesis. Bioessays 31, 1347-1356.

Seifert, A.W., Kiama, S.G., Seifert, M.G., Goheen, J.R., Palmer, T.M., Maden, M., 2012. Skin shedding and tissue regeneration in African spiny mice (Acomys). Nature 489, 561-565.

Sharpless, N.E., DePinho, R.A., 2007. How stem cells age and why this makes us grow old. Nat Rev Mol Cell Biol 8, 703-713.

Sousounis, K., Athippozhy, A.T., Voss, S.R., Tsonis, P.A., 2014a. Plasticity for axolotl lens regeneration is associated with age-related changes in gene expression. Regeneration (Oxf) 1, 47-57.

Sousounis, K., Baddour, J.A., Tsonis, P.A., 2014b. Aging and regeneration in vertebrates. Curr Top Dev Biol 108, 217-246.

Sousounis, K., Qi, F., Yadav, M.C., Millán, J.L., Toyama, F., Chiba, C., Eguchi, Y., Eguchi, G., Tsonis, P.A., 2015. A robust transcriptional program in newts undergoing multiple events of lens regeneration throughout their lifespan. Elife 4.

Suetsugu-Maki, R., Maki, N., Nakamura, K., Sumanas, S., Zhu, J., Del Rio-Tsonis, K., Tsonis, P.A., 2012. Lens regeneration in axolotl: new evidence of developmental plasticity. BMC Biol 10, 103.

Tsissios G., S.A., Chen W., Miller A., Wang H., Del Rio-Tsonis K., 2021. In vivo and ex vivo view of newt lens regeneration. In Salamanders: Methods in molecular biology (Clifton, N.J.) 2562:197-208 DOI: 10.1007/978-1-0716-2659-7_13.

Tsonis, P.A., Madhavan, M., Tancous, E.E., Del Rio-Tsonis, K., 2004. A newt's eye view of lens regeneration. Int J Dev Biol 48, 975-980.

Ver Hoef, J.M., Boveng, P.L., 2007. Quasi-Poisson vs. negative binomial regression: how should we model overdispersed count data? Ecology 88, 2766-2772.

Vergara, M.N., Tsissios, G., Del Rio-Tsonis, K., 2018. Lens regeneration: a historical perspective. Int J Dev Biol 62, 351-361.

Vinarsky, V., Atkinson, D.L., Stevenson, T.J., Keating, M.T., Odelberg, S.J., 2005. Normal newt limb regeneration requires matrix metalloproteinase function. Dev Biol 279, 86-98.

Warraich, U.E., Hussain, F., Kayani, H.U.R., 2020. Aging - Oxidative stress, antioxidants and computational modeling. Heliyon 6, e04107.

White, G.C., & Bennetts, R. E., 1996. Analysis of frequency count data using the negative binomial distribution. Ecology 77(8), 2549-2557.

Wood, S.N., 2006. Generalized additive models: an introduction with R. chapman and

hall/CRC.

Wood, S.N., 2022. mgcv: Mixed GAM Computation Vehicle with Automatic Smoothness Estimation. R package version 1.8-40.

Xiao, W., Chen, X., Li, W., Ye, S., Wang, W., Luo, L., Liu, Y., 2015. Quantitative analysis of injury-induced anterior subcapsular cataract in the mouse: a model of lens epithelial cells proliferation and epithelial-mesenchymal transition. Sci Rep 5, 8362.

Yamada, T., 1977. Control mechanisms in cell-type conversion in newt lens regeneration. Monogr Dev Biol 13, 1-126.

Yamada, T., McDevitt, D.S., 1974. Direct evidence for transformation of differentiated iris epithelial cells into lens cells. Dev Biol 38, 104-118.

Yamada, T., Roesel, M.E., 1969. Activation of DNA replication in the iris epithelium by lens removal. J Exp Zool 171, 425-432.

Yamada, T., Roesel, M.E., Beauchamp, J.J., 1975. Cell cycle parameters in dedifferentiating iris epithelial cells. J Embryol Exp Morphol 34, 497-510.

Yang, Y., Wang, T., Biswal, N.C., Wang, X., Sanders, M., Brewer, M., Zhu, Q., 2011. Optical scattering coefficient estimated by optical coherence tomography correlates with collagen content in ovarian tissue. J Biomed Opt 16, 090504.

Yee, T.W., & Mitchell, N. D., 1991. Generalized additive models in plant ecology. Journal of vegetation science 2(5), 587-602.

Yousefzadeh, M., Henpita, C., Vyas, R., Soto-Palma, C., Robbins, P., Niedernhofer, L., 2021. DNA damage-how and why we age? Elife 10.

Zalik, S.E., Yamada, T., 1967. The cell cycle during lens regeneration. J Exp Zool 165, 385-393.